WORLD CONFERENCE ON TIMBER ENGINEERING 2025
BRISBANE, AUSTRALIA
Advancing Timber for the Future Built Environment

EXPERIMENTAL INVESTIGATION ON THE PERFORMANCE OF NOVEL BOLTED GLULAM BEAM-TO-COLUMN CONNECTIONS UNDER THE COUPLING EFFECTS OF TENSION AND BENDING

Xuebing Zhao [1], **Xiaobin Song** [2]

ABSTRACT: This paper aims to improve the rotational capacity of bolted glulam beam-to-column connections under large deformation. Two novel connections were proposed: one with supplemental bolts and another with supplemental hold-downs. To simulate the stress condition of connections under large deformation, especially in the development of catenary action during progressive collapse. Monotonic tests considering the coupling effects of tension and bending were conducted on the four groups of specimens, including the conventional connections, connections reinforced with self-tapping screws, and two novel ones. Their failure modes and key performance parameters were analysed. The results showed that compared with the conventional connection, the ductility of the self-tapping screws-reinforced connection increased by 28%. The connection with supplemental bolts showed a significant improvement with a 158% increase in moment capacity and a 56% increase in maximum rotation over the conventional one. The connection with supplemental hold-downs reached the highest effective stiffness improvement at 59% compared to the conventional one.

KEYWORDS: glulam, bolted beam-to-column connection, performance, the coupling effect of tension and bending

1 – INTRODUCTION

Mass timber structures, valued for ease of assembly and aesthetics, commonly utilize bolted beam-to-column connections [1-5]. However, their low structural continuity and redundancy [6,7], make them prone to progressive collapse triggered by local connection failures [8,9], as evidenced by collapses at Ballerup Siemens-arena and Bad Reichenhall Ice-arena [10-12]. Connections critically influence structural robustness [13], but glulam bolted connections exhibit limited rotational capacity and ductility, hindering catenary action development during progressive collapse [13]. Thus, Lyu et al. made much effort to enhance the progressive collapse resistance of mass timber structures [13-14], but the rotational capacities of the connections still need to be improved. Additionally, current research [2-5] predominantly examines pure bending or shear-bending scenarios, neglecting the tension and bending coupling effect that emerges under large deformations when catenary action initiates.

Therefore, this study proposes two novel glulam bolted connections enhanced with supplemental bolts and hold-downs to improve rotational capacity. Four specimen groups were tested under combined tension-bending effects: conventional connections, self-screw-reinforced connections, and the two novel connections. Their performance was compared and evaluated through failure modes, moment-rotation curves, and key parameters.

2 – EXPERIMENT

2.1 CONNECTION DESIGN

Four groups of bolted glulam beam-column connections were designed: conventional (JDTB1), self-tapping screw-reinforced (JDTB2), supplemental bolt-enhanced (JDTB3), and hold-down-augmented (JDTB4). JDTB1 with two specimens comprised glulam members, slotted steel plates, and bolts. Employing common reinforcement method, JDTB2 with two specimens added eight 9×340 mm self-tapping screws (45 mm bolt-screw spacing) following [3,15]. Test consistency in JDTB1/JDTB2 enabled single-specimen testing for novel connections due to budget constraints. Inspired by Lyu et al.'s work [13], JDTB3 incorporated four supplemental bolts with arch-shaped holes (0.24 rad radius) to optimize large-deformation performance. JDTB4 employed prefabricated hold-downs secured by eight 5×70 mm screws and two 16 mm anchor bolts, with 50 mm oblong holes in the hold-

[1] Xuebing Zhao, Department of Structural Engineering, Tongji University, Shanghai, China, xuebing_zhao@tongji.edu.cn

[2] Xiaobin Song, Department of Structural Engineering, Tongji University, Shanghai, China, xiaobins@tongji.edu.cn

https://doi.org/10.52202/080513-0397

down to prevent premature screw shear. All supplemental components were supplied by the Rothoblaas®. The detailed dimensions of connections are shown in Fig. 1.

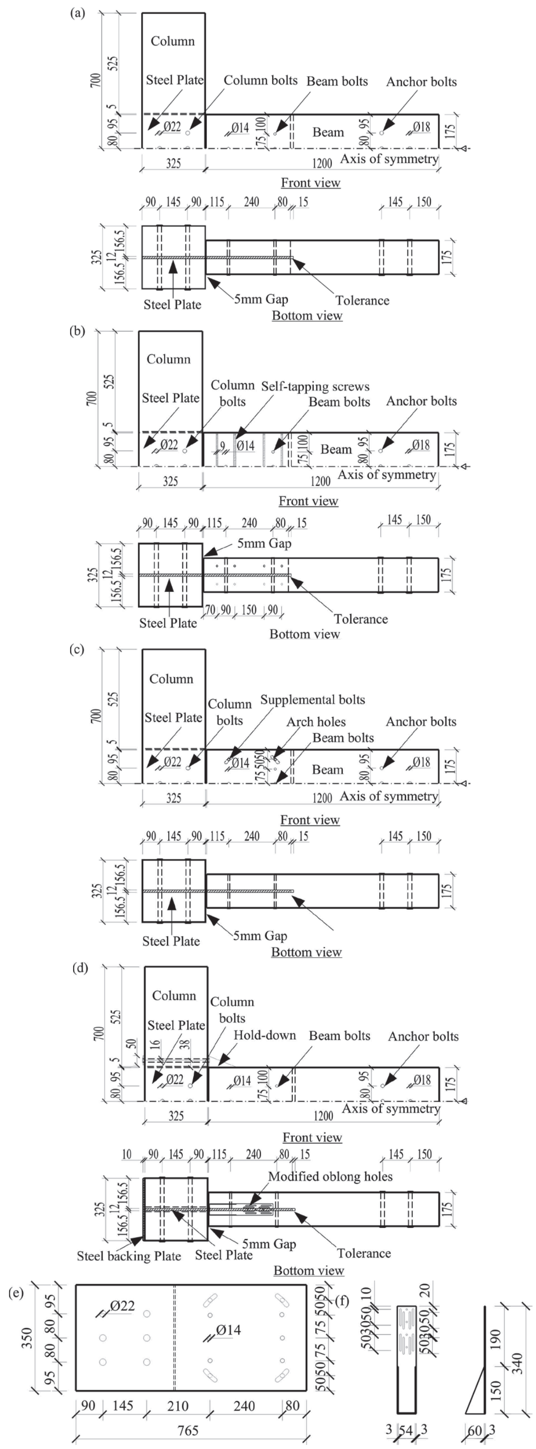

Figure 1. Detailed configuration and dimensions: (a) JDTB1; (b) JDTB2; (c) JDTB3; (d) JDTB4; (e) the steel plate with arch holes; and (f) the prefabricated hold-downs with oblong holes.

2.2 MATERIAL PROPERTIES

The glulam used North American Douglas fir (TC_T32 grade). Small clear samples were extracted to assess its material properties. As per GB/T 1927 [16] and ASTM D 143–14 [17], the average moisture content was 11.6%, with other properties in Table 1. The steel plates were made from 9.5 mm-thick Q345B grade steel plates following GB/T 50017 [18]. They were fixed in glulam grooves using 8.8-grade low-carbon steel hex bolts, with a nominal yield strength of 640 MPa, as per GB/T 1231 [19].

Table 1: Material properties of the glulam

Material property parameters	Mean value (MPa)	COV (%)
Parallel-to-grain compressive MOE	11070	9.14
Perpendicular-to-grain compressive MOE	721	7.22
Parallel-to-grain compressive strength	64.63	2.44
Perpendicular-to-grain compressive strength	4.02	9.16
Parallel-to-grain tensile strength	115.32	14.23
Perpendicular-to-grain tensile strength	2.39	18.22
Parallel-to-grain shear strength	12.56	5.96

2.3 TEST SETUP AND DATA MEASUREMENT

Tests were conducted in the Laboratory of Building Structures, Department of Structural Engineering, Tongji University, Shanghai, China. The setup included two adjustable steel reaction frames, a customized steel base, and a 200-kN hydraulic actuator with a 500-mm stroke (Fig. 2). To achieve the application of combined tension and bending, the specimens were rotated 90°. The beam end was fixed with a steel base and six 18-mm bolts. The actuator was mounted on the column via a rotatable cage.

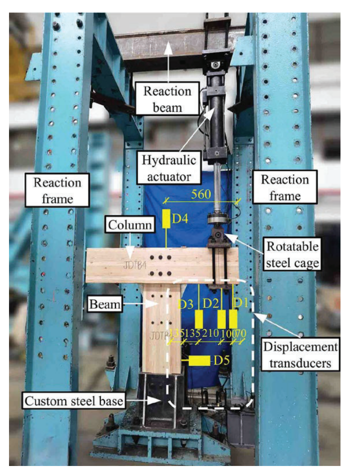

Figure 2. Test setup and data measurement scheme.

https://doi.org/10.52202/080513-0397

The loading protocol included preloading and formal loading phases. Preloading eliminated initial gaps and calibrated sensors. Formal loading continued at 5 mm/min until failure (20% load drop from peak or actuator stroke limit). As shown in Fig. 2, load was measured by the actuator's built-in load cell, while displacements were recorded using five transducers: D1 monitored vertical displacement at the column's free end, D2 tracked the loading point displacement, D3-D4 were attached to the column, and D5 captured horizontal rigid-body movement.

3 – RESULTS AND DISCUSSIONS

3.1 TYPICAL FAILURE MODES

After disassembling connections, six anchor bolts in the customized base were found to be straight with no obvious deformation, indicating a reliable fixed end. The typical failure modes of each group are as follows.

JDTB1-2: As shown in Fig. 3, three transverse beam cracks developed in the beam, with no obvious column cracks. Column bolts near the actuator slightly deformed. Three beam bolts in the lower row experienced significant deformation, and a total of three bolts fractured.

JDTB2-2: As depicted in Fig. 4, Only two cracks appeared in the beam-column region, and the embedment of self-tapping screws with the wood's local failure implied the function of the self-tapping screws. Column bolt deformation was similar to JDTB1-2. However, the plastic deformation of beam bolts was less severe, but four middle and right bolts fractured due to large displacement.

JDTB3: As shown in Fig. 5, Upon reaching (0.7 ~ 0.8) F_u (ultimate load), four supplemental bolts in the arched holes activated. When loaded to (0.8 ~ 0.9) F_u, tensile region supplemental bolts reached arch edges, causing longitudinal cracks, wood shear failure, and significant fibre rupture. After disassembling, four column bolts near the actuator presented significant plastic deformation, and most of the beam bolts fractured.

JDTB4: As shown in Fig. 6, Upon reaching approximately 0.7 F_u, the self-tapping screws of the hold-down in the tensile region reached the edge of oblong holes, leading to successive fractures. Three primary cracks eventually developed in the beam, with wood shear failure and extensive wood embedment. Bolt deformations in both beam and column were similar to JDTB1-2. Only one lower row beam bolt fractured, and the tensile region hold - down deformed more.

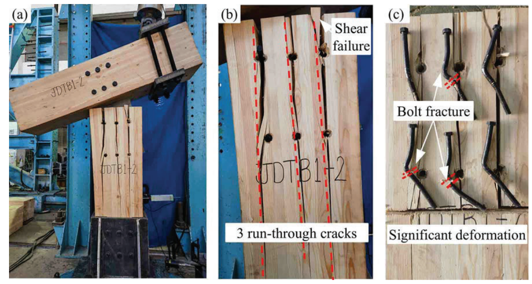

Figure 3. Typical failure modes of JDTB1-2: (a) overall failure; (b) ultimate failure of the beam; and (c) deformation of the beam bolts.

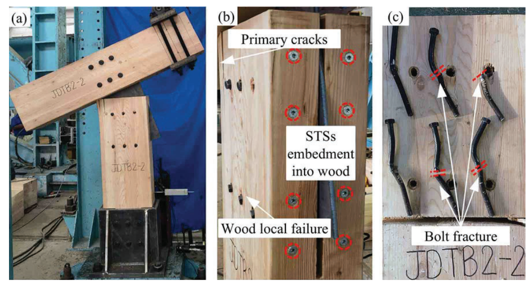

Figure 4. Typical failure modes of JDTB2-2: (a) overall failure; (b) ultimate failure of the beam; and (c) deformation of the beam bolts.

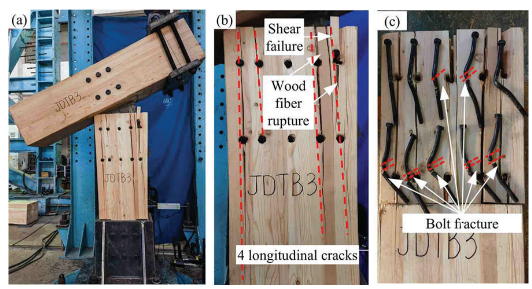

Figure 5. Typical failure modes of JDTB3: (a) overall failure; (b) ultimate failure of the beam; and (c) deformation of the beam bolts.

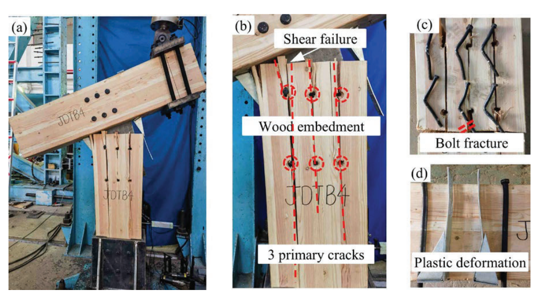

Figure 6. Typical failure modes of JDTB4: (a) overall failure; (b) ultimate failure of the beam; (c) deformation of the beam bolts; and (d) deformation of the hold-downs.

3.2 MOMENT-ROTATION RESPONSE

To evaluate the rotational capacity of the connections, obtaining their moment-rotation response is crucial. The moment (M) and the relative rotation of the column to the beam (θ) can be determined as follows:

$$M = FH \tag{1}$$

$$\theta = \arctan[\frac{D_3 - D_4}{270}] \tag{2}$$

Where F denotes the vertical load applied by the actuator; H is the distance from the load point to the centre of the glulam bolts (450 mm for JDTB1 and JDTB2-1, 525 mm for others); D_3 and D_4 are the readings from transducer D3 and D4 (270 mm apart), respectively.

Fig. 7 shows the moment-rotation response. All specimens experienced three phases: linear elastic (I), inelastic (II), and failure at large deformation (III). As per UFC 4-023-03 [20], connections enter the large deformation phase at a rotation of 11.5°. It should be noted that as the bearing capacity of JDTB2-1 showed no obvious decrease when reaching 85% of the maximum capacity of the actuator, leading to the test being stopped. Thus, its loading process was incomplete. Due to resource limits, the load point was moved 75 mm outward for other connections. A retest of JDTB2-1 confirmed the adjustment's validity.

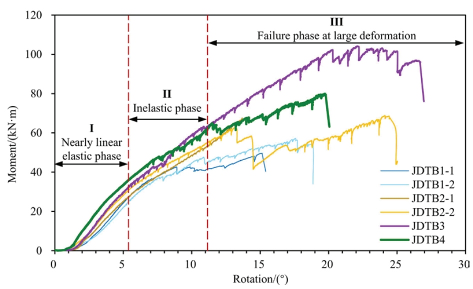

Figure 7. Moment-rotation response of each group.

3.3 KEY PERFORMANCE PARAMETERS

To compare the rotational capacity of four connections, key performance parameters were analysed. Due to varying M-θ responses, definitions for key points were introduced: the initial moment drop was defined as the plastic moment (M_p), with the corresponding rotation as the plastic rotation (θ_p). The ultimate moment (M_u) was defined as the point where the moment dropped to 80% of its peak or the load decreased rapidly, corresponding to rotation (θ_u). The Yasumura & Kawai method [21] was used to determine the key performance parameters.

As shown in Fig. 7 and Table 2, JDTB2 had the highest ductility increase rate of 28%, though the improvement in moment capacity and stiffness was modest. Compared with JDTB1, JDTB3's ultimate moment and rotation increased by 158% and 57%, respectively. However, its initial elastic stiffness was similar to JDTB1. These ratios showed that supplemental bolts were ineffective initially but effective in large deformation, validating the design. Despite a smaller ultimate rotation increase, JDTB4 matched JDTB3 in other properties. Its initial stiffness and effective stiffness were 29% and 59% higher than JDTB1, due to the supplemental hold-downs.

4 – CONCLUSIONS

This paper experimentally studied novel bolted glulam beam-column connections under tension and bending. The main conclusions are as follows:

(1) Conventional connections failed with transverse cracks, plug shear, and bolt fractures. Self-tapping screws restrained cracks. Connections with supplemental bolts or hold-downs had similar failure modes but with more severe cracks and beam bolt deformation.

Table 2: Comparative analysis of key performance parameters of various connections.

Specimen ID	Stiffness		Yield state		Plastic state		Ultimate state		Ductility
	K_i (kN·m/°)	K_e (kN·m/°)	M_y (kN·m)	θ_y (°)	M_p (kN·m)	θ_p (°)	M_u (kN·m)	θ_u (°)	μ
JDTB1	7.12	3.11	33.05	6.30	50.04	16.04	37.15	17.19	2.63
JDTB2	7.17	3.93	40.65	7.45	54.77	13.75	45.01	25.21	3.38
Change ratio	1%	26%	23%	18%	9%	-14%	21%	47%	29%
JDTB3	7.18	4.65	45.57	8.02	99.5	21.20	96	26.93	3.32
Change ratio	1%	49%	38%	27%	99%	32%	158%	57%	26%
JDTB4	9.18	4.94	43.53	6.88	60.15	12.03	63.16	20.05	2.96
Change ratio	29%	59%	32%	9%	20%	-25%	70%	17%	13%

https://doi.org/10.52202/080513-0397

Note: The values for JDTB1 and JDTB2 represent the average values of their respective two specimens; K_i is the initial elastic stiffness, calculated as $K_i = \frac{40\%M_p - 10\%M_p}{40\%\theta_p - 10\%\theta_p}$; K_e is the effective stiffness, calculated as the ratio of the plastic moment (M_p) to the corresponding rotation (θ_p); M_y, M_p, and M_u represent the yield moment, plastic moment, and ultimate moment, respectively, along with their respective rotations θ_y, θ_p, and θ_u; μ is the ductility coefficient, calculated as $\mu = \frac{\theta_u}{\theta_y}$

(2) All specimens underwent three phases: nearly linear elastic, inelastic, and failure at large deformation.

(3) The self-tapping screw connection saw the highest ductility increase at 28%. The supplemental bolt connection's ultimate moment and rotation rose by 158% and 57%. The supplemental hold-down connection had a 17% ultimate rotation increase, with initial and effective stiffness improvements of 29% and 59% over the conventional one.

In conclusion, connections with self - tapping screws and supplemental bolts had preferable rotational capacity, potentially offering enough rotation for catenary action. The supplemental hold-down connection needs refinement. Further parametric numerical analysis is required for connection refinement and a comprehensive theoretical design approach.

5 – ACKNOWLEDGEMENT

The authors gratefully acknowledge the financial support from the National Natural Science Foundation of China. (Grant No. 52178243).

6 – REFERENCES

[1] J. Tollefson. "The wooden skyscrapers that could help to cool the planet." In: Nature 545 (2017), pp. 280-282.
[2] M. Q. Wang, X. B. Song, X. L. Gu, Y. F. Zhang, and L. Luo. "Rotational Behavior of Bolted Beam-to-Column Connections with Locally Cross-Laminated Glulam." In: Journal of Structural Engineering 141.4 (2015), pp. 04014121.
[3] M. J. He and H. F. Liu. "Comparison of glulam post-to-beam connections reinforced by two different dowel-type fasteners." In: Construction and Building Materials 99 (2015), pp. 99-108.
[4] X. B. Song, Y. R. Ma, X. L. Gu, and M. Q. Wang. "Carbon Fiber–Reinforced Polymer Reinforcement for Rotational Behavior of Bolted Glulam Beam-to-Column Connections." In: Journal of Composite for Construction 21.3 (2017), pp. 04016096.
[5] X. F. Sun, L. Luo, S. Sun, J. Luo, and J. J. Ou. "An experimental and numerical study on the rotational behavior of bolted glulam beam-to-column connections reinforced by double U-shaped welded steel sections." In: Engineering Structures 301 (2024), pp. 117315.
[6] B. Abdelwahed. "A review on building progressive collapse, survey and discussion." In: Case Studies in Construction Materials 11 (2019), pp. e00264.
[7] N. Elkady, L. A. Nelson, L. Weekes, N. Makoond, and M. Buitrago. "Progressive collapse: Past, present, future and beyond." In: Structures 62 (2024), pp. 106131.
[8] S. M. Marjanishvili. "Progressive Analysis Procedure for Progressive Collapse." In: Journal of Performance of Constructed Facilities 18.2 (2004), pp. 79-85.
[9] ASCE. "Minimum Design Loads for Buildings and Other Structures." (2013).
[10] M. Hansson and H. J. Larsen. "Recent failures in glulam structures and their causes." In: Engineering Failure Analysis 12.5 (2005), pp. 808-818.
[11] E. Frühwald Hansson. "Analysis of structural failures in timber structures: Typical causes for failure and failure modes." In: Engineering Structures 33 (2011), pp. 2978-2982.
[12] J. M. Cabrero, B. Iraola, and M. Yurrita. "Failure of timber constructions." In: Handbook of Materials Failure Analysis, Elsevier, (2018).
[13] C. H. Lyu, B. P. Gilbert, H. Guan, I. D. Underhill, S. Gunalan, H. Karampour, and M. Masaeli. "Experimental collapse response of post-and-beam mass timber frames under a quasi-static column removal scenario." In: Engineering Structures 210 (2020), pp. 110562.
[14] C. H. Lyu, B. P. Gilbert, H. Guan, I. D. Underhill, S. Gunalan, and H. Karampour. "Experimental study on the quasi-static progressive collapse response of post-and-beam mass timber buildings under corner column removal scenarios." In: Engineering Structures 242 (2021), pp. 112497.
[15] Eurocode 5. "Design of timber structures. Part 1-1. General. Common rules and rules for buildings." (2004).
[16] GB/T 1927. "Test methods for physical and mechanical properties of small clear wood specimens." (2022). (in Chinese)
[17] ASTM D 14. "Conventional test methods for small clear specimens of timber" (2014).
[18] GB/T 50017. "Code for design of steel structures." (2003). (in Chinese)
[19] GB/T 1231. "Specifications of high strength bolts with large hexagon head, large hexagon nuts, plain washers for steel structures" (2006). (in Chinese)
[20] DoD. "UFC 4-023-03 Design of buildings to resist progressive collapse" (2016).
[21] M. Yasumura and N. Kawai. "Estimating seismic performance of wood-framed structures." In: Proceedings of 5th WCTE 2 (1998), pp. 564-571.